Direct radiative capture of p-wave neutrons

A. Mengoni,[1,2] T. Otsuka,[2,3] and M. Ishihara[2,3]

[1] *ENEA, Applied Physics Section, V.le G. B. Ercolani 8, I-40138 Bologna, Italy*

[2] *RIKEN, Radiation Laboratory, 2-1 Hirosawa, Wako, Saitama 351-01, Japan*

[3] *The University of Tokyo, Department of Physics, Hongo, Bukyo-ku, Tokyo 113, Japan*

(August 11, 1995)

Abstract

The neutron direct radiative capture (DRC) process is investigated, highlighting the role of incident p-wave neutrons. A set of calculations is shown for the ^{12}C(n,γ) process at incoming neutron energies up to 500 keV, a crucial region for astrophysics. The cross section for neutron capture leading to loosely bound s, p and d orbits of ^{13}C is well reproduced by the DRC model demonstrating the feasibility of using this reaction channel to study the properties of nuclear wave functions on and outside the nuclear surface. A sensitivity analysis of the results on the neutron-nucleus interaction is performed for incident s- as well as p-waves. It turned out that the DRC cross section for p-wave neutrons is insensitive to this interaction, contrary to the case of incident s-wave neutrons.

PACS number(s): 25.40Lw,21.10Gv,23.40.Hc

The direct radiative capture (DRC) process of neutrons in the keV energy region has some peculiarity recently revived by theoretical analysis [1] as well as by new experimental results [2–4]. Because of the non-resonant nature of the DRC process, the complications related to the calculation of the compound nucleus wave function in the entrance channel are removed. This is a general feature of all the direct capture processes, including those induced by charged particle reactions. However, because of the lack of the Coulomb interaction, the (n,γ) reaction has salient features which makes it a unique probe for investigating nuclear structure information. In fact, the neutron capture process can be explored in the very low neutron energy region where the reaction mechanism may be fully decoupled from the resonance process. In this way, precise information can be obtained for the structure of the capturing orbit and the relative contribution of the various l-wave components to the cross section can be examined separately.

Because the DRC process is essentially taking place on the nuclear surface and in the external region, it has been recently proposed [1] to use this reaction channel to study the properties of nuclear wave functions, in connection with the discovery of the neutron halo of light drip-line nuclei [6]. The same kind of information can also be derived from the inverse reaction channel (Coulomb dissociation) where a strong enhancement of the low-lying dipole mode has been observed [5] and treated as an inverse DRC process [1].

While the DRC of protons and alpha particles have been widely investigated in the energy range from a few hundreds of keV up to several MeV [7], the DRC process of neutrons has been mainly examined at thermal (E_n = 0.0253 eV) energies where s-wave neutrons are captured into bound p orbits. The DRC formalism for thermal neutrons has been revised by Raman *et al.* [8]. They have shown in detail how the neutron-nucleus potential strongly affects the capture mechanism of s-wave neutrons in light nuclei, whereas no reference to high energy extension nor to higher partial-wave (including p-waves) contributions was given. On the other hand, we may expect that, as the incoming neutron energy increases the capture of p-wave neutrons into bound s and d orbits comes into play and, under proper conditions, it can be regarded as the dominant capture process.

The extension of the capture models required to include p-waves and higher partial waves into the neutron DRC process is the main task of this note. In addition, a sensitivity analysis of the DRC process to the neutron-nucleus potential for energies in the keV region will be performed. We stress that applications of DRC models have been rarely extended to energies higher than thermal. In nuclear astrophysics there have been several applications at neutron energies of interest in the r-process nucleosynthesis [9] and for inhomogeneous big-bang theories [10]. For such kind of applications it is necessary to assess quantitatively the DRC prescriptions in a range of energies from a few up to several hundreds of keV.

Here we will briefly revise the DRC model for s- and p-wave neutrons and apply it to the calculation of the ^{12}C(n,γ) cross sections for transitions leading to all the four bound states of ^{13}C . In particular we will consider realistic wave functions for the initial scattering state and we will focus the attention on the influence of the initial l-wave character on the capture cross section.

In the early works on neutron capture reactions [11–14] it was recognized that a capture mechanism, in which the incoming neutron is scattered directly into a final bound state without forming a nuclear compound state, might take place for nuclei where the final state is dominated by a strong single-particle configuration. There have been several formulations of the DRC mechanism differing considerably among each other in the way the incoming channel and the final state are described [13,15,8,1]. In general, because the direct capture process is alternative to the compound nucleus (CN) formation mechanism, we can separate the collision matrix into two components

$$U_{i\to f} = U_{i\to f}(CN) + U_{i\to f}(DRC) \tag{1}$$

where all the quantum numbers necessary to define the initial and final states have been lumped into the notation i and f, respectively. The reaction cross section is given by

$$\sigma_{i\to f} = \frac{\pi}{k^2}|U_{i\to f}|^2 \tag{2}$$

where k is the wave number of the relative motion in the entrance channel. Here we will

deal only with the DRC part of the collision matrix. The capture cross section for emission of electric dipole radiation (E1) in the transition $i \to f$ is given by

$$\sigma_{n,\gamma} = \frac{16\pi}{9\hbar} k_\gamma^3 \bar{e}^2 |\, Q_{i\to f}^{(1)}\,|^2 \tag{3}$$

where $k_\gamma = \epsilon_\gamma/\hbar c$ is the emitted γ-ray wave number corresponding to the γ-ray energy ϵ_γ and $\bar{e} = -eZ/A$ is the E1 effective charge for neutrons. The cross section is, therefore, essentially determined by the matrix elements

$$Q_{i\to f}^{(1)} = < \Psi_f | \hat{T}^{E1} | \Psi_i > \tag{4}$$

where $\hat{T}^{E1} = rY^{(1)}(\theta,\phi)$ is th electric dipole operator. Here, the initial state wave-function Ψ_i is given by a unit-flux incoming wave in the entrance channel, scattered at the origin by the neutron-nucleus potential. The final state wave-function Ψ_f is given by the residual nucleus (bound) final state. The radial coordinate r denotes the distance of the incoming neutron with respect to the target nucleus.

The entrance channel wave function can be decomposed into spherical (l-wave) components

$$\Psi_{lm}(\mathbf{r}) \equiv w_l(r) \frac{Y_{l,m}(\theta,\phi)}{rv^{1/2}} \tag{5}$$

where $w_l(r)$ depends also on the wave number k and is written, as usual, as

$$w_l(r) = \frac{i\sqrt{\pi}}{k}\sqrt{2l+1}\, i^l [I_l - U_l O_l]. \tag{6}$$

Here, the common notation for the asymptotic forms of the incoming and outgoing waves, respectively I_l and O_l, has been adopted

$$I_l \sim \exp(-ikr + \frac{1}{2}il\pi) \quad \text{and} \quad O_l \sim \exp(+ikr - \frac{1}{2}il\pi). \tag{7}$$

U_l indicates the collision matrix for the scattering process in the entrance channel, v is the incoming neutron velocity and k the corresponding wave number.

The matrix elements can be decomposed into the product of three factors $Q_{i\to f}^{(1)} = \mathcal{I}_{if} \cdot A_{if} \cdot \sqrt{S}$.

Radial part: Indicating with $u_{l_f}(r)$ the radial part of the final state wave function, the radial overlap integral is given by

$$\mathcal{I}_{l_i l_f} \equiv \int_0^\infty u_{l_f}(r) r w_{l_i}(r) dr. \tag{8}$$

If the final state wave function is dominated by a single-particle configuration with a long tail outside the nuclear radius (halo), there will be a strong effect on $\mathcal{I}_{l_i l_f}$ [1]. This will be shown below in the case of incoming s- and p-wave neutrons. Analytical expressions for $\mathcal{I}_{l_i l_f}$ can be derived for specific assumptions on the initial and final state wave functions. If a hard-sphere model for the scattering wave function and a crude square-well model for the bound p orbital are assumed for the initial and final state respectively one recovers the very well known [13] expression for the hard-sphere capture cross section

$$\sigma_{n,\gamma}^{HS} = \frac{32\pi}{3} \; k_\gamma^3 \; \frac{\bar{e}^2}{\hbar v} \frac{R^5}{y^4} (\frac{3+y}{1+y})^2 \tag{9}$$

where $y \equiv \chi R$. Here, χ is the reciprocal attenuation length of the wave function tail given by $\chi = \sqrt{2\mu S_n}/\hbar$, where μ is the reduced mass of the system and S_n the neutron separation energy from the residual state. More elaborate expressions corresponding to different assumptions on the initial and final state wave functions, can be derived for this overlap integral and they can be found in the literature [13,8,16].

Angular part: For a general $l_i \rightarrow l_f$ transition, the angular factor which takes into account the magnetic degeneracy of the final state and is averaged over the initial magnetic substates is given by

$$A_{l_i l_f}^2 \equiv \frac{1}{2l_i+1} |\langle l_f \| \hat{Y}_1 \| l_i \rangle|^2 = \frac{3}{4\pi} (l_i 010 | l_f 0)^2 \tag{10}$$

where $(....|..)$ is a Clebsh-Gordan coefficient. The orbital angular momentum, $\mathbf{l}$, can couple with the intrinsic spin, $\mathbf{s}$, to give the angular momentum $\mathbf{j} = \mathbf{l} + \mathbf{s}$. The corresponding $\mathbf{j}_i$ and $\mathbf{j}_f$ can be combined with the target spin $\mathbf{I}$ to obtain the initial and final state total angular momenta $\mathbf{J}_i$ and $\mathbf{J}_f$. The angular-spin coefficient for the full coupling is given by

$$A_{if}^2 \equiv \frac{|\langle J_f, I, j_f \| \hat{Y}_1 \| J_i, I, j_i \rangle|^2}{2J_i+1} = \frac{3}{4\pi}(2l_i+1)(2j_i+1)(2j_f+1)(2J_f+1) \times$$

$$\times (l_i 010|l_f 0)^2 \ \left\{ \begin{matrix} j_i & I & J_i \\ J_f & 1 & j_f \end{matrix} \right\}^2 \left\{ \begin{matrix} l_i & 1/2 & j_i \\ j_f & 1 & l_f \end{matrix} \right\}^2 \qquad (11)$$

where $\{...\}$ are Wigner-6j coefficients.

Final state strength: The single particle strength, S, of the final-state orbit is usually derived from (d,p) stripping reactions (spectroscopic factor). We note here that if the radial part of the matrix elements, Eq. (8), is calculated with reliable wave functions (see below) the spectroscopic factor can be derived from a DRC analysis of the experimental cross section. This technique, proposed and applied in proton capture reactions [7], could be applied in the neutron capture channel with the advantages already noted above.

For thermal neutrons, the main contribution to the capture process is due to incoming s-wave neutrons captured into p-wave orbits and emitting E1 radiation. At higher neutron energy, however, the incoming p-wave neutrons come into play as they can be captured into bound s and d orbits. In ^{13}C both these even parity orbits are available. Moreover their respective levels have the characteristics of being loosely bound and with large spectroscopic strengths: they are good example of halo structure in excited states of stable nuclei. The nuclear structure information on ^{13}C are summarized in Table I.

Before showing the result of the full $^{12}\mathrm{C}(n,\gamma)$ cross section calculations we will show here how the s- and p-wave neutron capture is affected by the neutron-nucleus potential.

For the purpose of the present study it is sufficient to consider single particle wave functions for the bound-state orbits of ^{13}C. They have been calculated using a Wood-Saxon potential with a radius parameter $r_0 = 1.236$ fm, a diffuseness $d = 0.62$ fm and a spin-orbit potential strength $V_s = 7$ MeV. The potential well depths were adjusted so as to reproduce the correct binding of the four bound states in terms of the corresponding single particle orbits. In the case of the $2s_{1/2}$ state this gives rise to $V_0 = 59.23$ MeV.

In the present investigation we have treated the incoming neutron channel with the following approximations:

(a) plane wave (PW) approximation

$$U_l = 1 \qquad \text{for all } l$$

(b) hard-sphere (HS): scattering by an infinitely deep potential well of radius R

$$\begin{aligned} U_l &= e^{-2ikR} && \text{for } l = 0 \\ &= e^{-2ikR} \times \tfrac{1+ikR}{1-ikR} && \text{for } l = 1 \end{aligned}$$

(c) a general case in which the collision matrix is calculated numerically for a given potential of Wood-Saxon form.

In order to see the effect of these three different treatments on the radial part of the matrix elements we show in Figs. 1 and 2 the calculation of the integrand of $\mathcal{I}_{if}$ in Eq. (8) at $E_n = 200$ keV. Because of its dominant contribution to the integral, only the real (imaginary) part is shown in Fig. 1 (2) for s- (p-) wave capture. The cross section is proportional to the squared area under the curves shown in the figures.

From Fig. 1 it is evident that for an initial s-wave state the result is strongly dependent on the neutron-nucleus potential adopted, namely on the different collision matrix of the scattering channel used in the calculation. Moreover, the behavior of the wave function inside the nuclear radius may result in a significant cancelation of the radial matrix element. This result is in full agreement with the conclusions of a detailed study of the thermal capture in light nuclei by Lynn *et al.* [17]. We believe that this sensitivity is the main source for discrepancy observed between the calculated and experimental thermal cross sections in DRC model analysis. The influence of compound nucleus components in the collision process is, naturally, another source of uncertainty.

On the contrary, for incoming p-wave neutrons, the radial matrix elements are essentially insensitive to the different collision matrices considered. This is evident, from Fig. 2, for both the $p \rightarrow s$ and the $p \rightarrow d$ transitions. In other words, in a situation where the capture is dominated by a DRC process of p-wave neutrons, the cross section is not sensitive

to the neutron-nucleus potential. Hence, the capture process is essentially determined by the structure of the *final* state wave function. In particular, the component of the wave function outside the nuclear radius plays the principal role in the determination of the capture strength. This is the main result of the present investigation.

The results of the full calculation of the capture cross section for transitions leading to the four bound states in ^{13}C are shown in Figs. 3 and 4.

In Fig. 3, the capture cross sections for transitions leading to the ground state (upper part) and to the level at E_x = 1.26 MeV (lower part) are shown. The curves labeled by (a), (b) and (c) refer to three different scattering wave functions calculated according to the three treatments (PW, HS and diffused Wood-Saxon potential) described above. For these two transitions, incoming s- and d-wave neutrons are involved in composing the initial state wave function. The large discrepancy between the experimental values and the calculation is removed only if a realistic neutron-nucleus potential is employed in the calculation. In our case, such an agreement was obtained when the same potential used for the bound-state calculation was employed (curve (c) in the figure). This is an important point because the obtained wave functions might have had unphysical overlaps and should have been orthogonalized if different potentials would have been used.

We have extended the calculations down to thermal energy (E_n = 0.0253 eV) using the same Wood-Saxon potential and the results are shown in Table I. Considering that no adjustment of any parameter was performed, the results of our DRC calculation can be considered satisfactory.

The relative contribution of incoming d-waves can be seen in Fig. 3. There, the dotted lines show the contribution of the s-wave capture component only, whereas the full line (c) show the contribution of both s- and d-wave components. Thought not decisively, the experimental results seem to follow the increasing trend due to the onset of the higher partial wave component.

Finally, the cross sections for transitions leading to the $s_{1/2}$ and $d_{5/2}$ orbits are shown in Fig. 4. These are the transitions due to the capture from p-wave neutrons. A very

good agreement is found for both the reaction channels, implying reliability of the DRC mechanism in the energy region under consideration. In this figure the conclusion drawn above from the radial matrix elements calculations can be verified explicitly. The results of the calculations obtained using the PW, HS or the full Wood-Saxon potential are barely distinguishable. No major influence of the neutron-nucleus potential used is revealed by the calculations, very well supported by the experimental results.

In summary, our calculations have shown that, while the DRC process of s-wave neutrons is strongly biased by the incoming-neutron interaction with the target, the DRC of p-wave neutrons is essentially insensitive to the details of this interaction. This fact can be used to derive important nuclear structure information on the residual nucleus like "exotic" components of the neutron wave function outside the nuclear radius (i.e. neutron halo) or single particle strength (spectroscopic factor) of the final capturing state.

We acknowledge many fruitful discussions with Y. Nagai and C. Coceva. This work has been supported in part by Grant-in-Aid for Scientific Research on Priority Areas (No. 05243102).

REFERENCES

[1] T. Otsuka, M. Ishihara, N. Fukunishi, T. Nakamura and M. Yokoyama, Phys. Rev. C **49**, R2289 (1994).

[2] Y. Nagai, M. Igashira, N. Mukai, T. Ohsaki, F. Uesawa, K. Takeda, T. Ando, H. Kitazawa, S. Kubono and T. Fukuda, Ap. J. **381**, 444 (1991).

[3] T. Ohsaki, Y. Nagai, M. Igashira, T. Shima, K. Takeda, S. Seino and T. Irie, Ap. J. **422**, 912 (1994).

[4] M. Igashira, Y. Nagai, K. Masuda, T. Ohsaki and H. Kitazawa, Ap. J. **441**, L89 (1995).

[5] T. Nakamura *et al.*, Phys. Lett. B **331**, 296 (1994).

[6] I. Tanihata, H. Hamagaki, O. Hashimoto, Y. Shida, N. Yoshikawa, K. Sugimoto, O. Yamakawa and N. Takahashi, Phys. Rev. Lett. **55**, 2676 (1985); I. Tanihata, Nucl. Phys. **A522**, 275c (1991).

[7] J. D. King, R. E. Azuma, J. B. Vise, J. Görres, C. Rolfs, H. P. Trautvetter and A. E. Vlieks, Nucl. Phys. **A567**, 354 (1994); references therein.

[8] S. Raman, R. F. Carlton, J. C. Wells, E.T. Jurney, and J. E. Lynn, Phys. Rev. C **32**, 18 (1985).

[9] G. J. Mathews, A. Mengoni, F. K. Thielemann and W. A. Fowler, Ap. J. **270**, 740 (1983).

[10] M. Wiesher, J. Görres and F. K. Thielemann, Ap. J. **363** 340 (1990).

[11] R. G. Thomas, Phys. Rev. **84**, 1061 (1951). [This is the oldest reference that we have found on the subject.]

[12] H. Morinaga and C. Ishii, Prog. Theor. Phys. **23**, 161 (1960).

[13] A. M. Lane and J. E. Lynn, Nucl. Phys. **17**, 563 (1960); **17**, 686 (1960).

[14] J. E. Lynn, *The theory of neutron resonance reactions* (Clarendon Press, Oxford, 1968).

[15] A. M. Lane and S. F. Mughabghab, Phys. Rev. C **10**, 417 (1974).

[16] A. Mengoni, T. Otsuka and M. Ishihara, in *Proceedings of a Specialists' Meeting on Measurement, Calculation and Evaluation of Phototn Production Data, Bologna, 1994*, edited by C. Coceva, A Mengoni and A. Ventura, (NEA/DOC/95/1), p. 185.

[17] J. E. Lynn, S. Kahane, and S. Raman, Phys. Rev. C **35**, 26 (1987).

[18] F. Ajzenberg-Selove, Nucl. Phys. **A523**, 1 (1991).

[19] S. F. Mughabghab, M. Divadeenam and N. E. Holden, *Neutron Cross Sections*, (Academic, New York, 1981), Vol. 1.

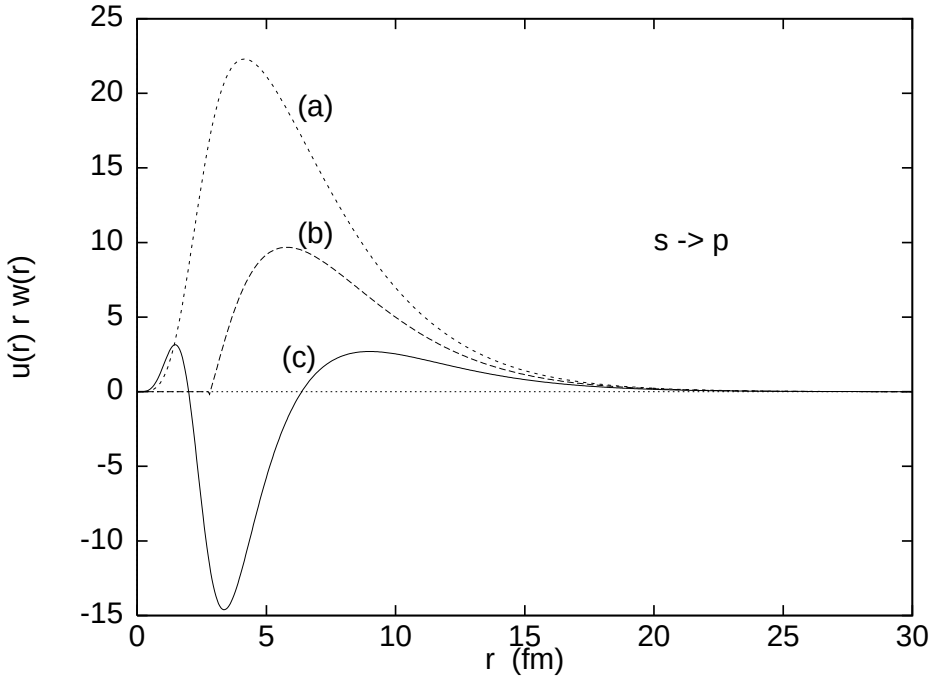

FIG. 1. Real part of the integrand of Eq. (8) for incoming s-wave neutrons of 200 keV and for the $1p_{3/2}$ orbit bound by 4.96 MeV. The scattering wave function $w(r)$ has been calculated according to (a) PW, (b) HS and (c) Wood-Saxon potential prescriptions. See the text for parameters and a detailed explanation.

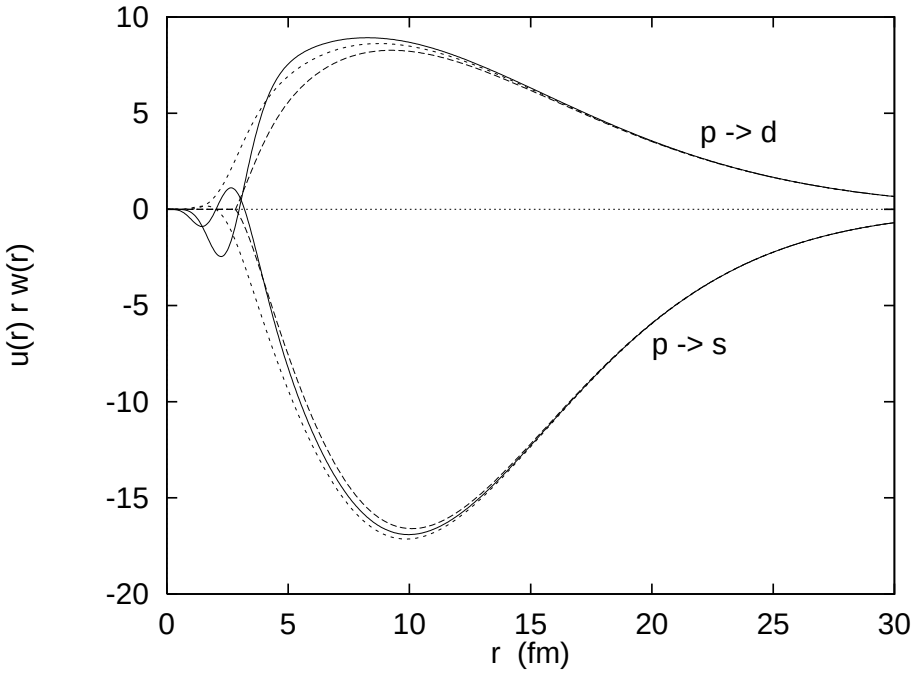

FIG. 2. Imaginary part of the integrand of Eq. (8) for incoming p-wave neutrons of 200 keV and for the $2s_{1/2}$ and $1d_{5/2}$ orbits bound by 1.86 and 1.09 MeV respectively. The scattering wave functions $w(r)$ have been calculated according to a PW (dashed line), HS (dotted line) and Wood-Saxon potential prescriptions (solid line). See the text for parameters and a detailed explanation.

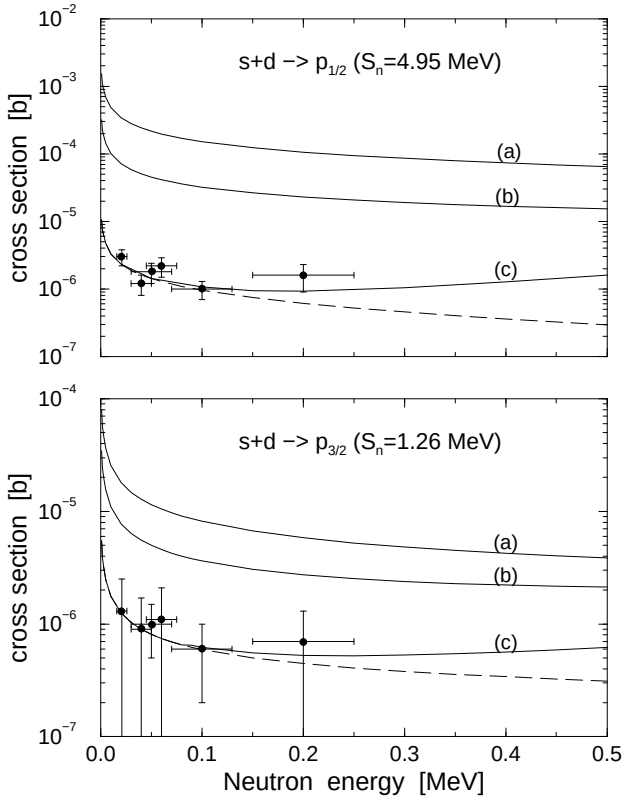

FIG. 3. Neutron capture cross section of ^{12}C for transitions leading to the ground state of ^{13}C (*upper part*) and to the level at $E_x = 3.684$ MeV (*lower part*). The experimental values are from the reference [2]. The curves labeled with (a), (b) and (c) correspond to the three different assumptions concerning the collision matrix for the scattering channel. See Figs. (1) and text for explanation. The dashed-line represents exclusively s-wave contribution to the capture.

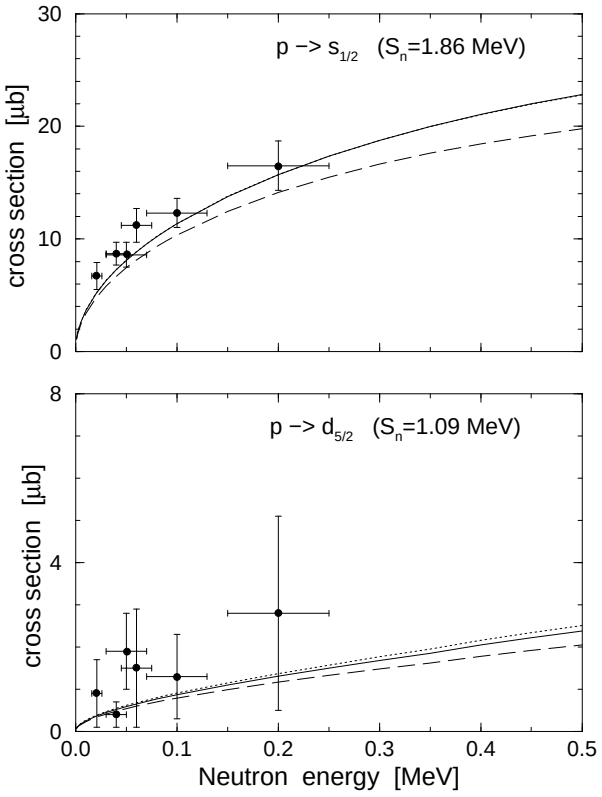

FIG. 4. Neutron capture cross section of ^{12}C for transitions leading to the $s_{1/2}$ orbit (*upper part*) and to the $d_{5/2}$ orbit of ^{13}C (*lower part*). The experimental values are from Ref. [2]. The dashed-, dotted- and solid-line correspond to the three different assumptions concerning the collision matrix for the scattering channel. See Fig. (2) and text for explanations. In this case, the capture is due to incoming p-wave neutrons only.

TABLES

TABLE I. Nuclear structure information of ^{13}C and thermal neutron capture cross section of ^{12}C.

E_x (MeV)	S_n (MeV)	l_n	$J\pi$	S_{dp} [a]	$\sigma^{th}_{n,\gamma}$ (mb)
0.0	4.946	1	1/2−	0.77	2.10
3.089	1.857	0	1/2+	0.65	-
3.684	1.262	1	3/2−	0.14	1.10
3.854	1.093	2	5/2+	0.58	-
Total					3.20
Experimental					3.53 ± 0.07 [b]

[a]From Ref. [18]

[b]From Ref. [19]